International Journal of
Molecular Sciences

MDPI

Article

Cx43 Hemichannel and Panx1 Channel Modulation by Gap19 and ^{10}Panx1 Peptides

Alessio Lissoni †, Siyu Tao †, Rosalie Allewaert, Katja Witschas *,‡ and Luc Leybaert *,‡

Department of Basic and Applied Medical Sciences—Physiology Group, Ghent University, 9000 Ghent, Belgium; alessio.lissoni@ugent.be (A.L.); siyu.tao@ugent.be (S.T.); rosalie.allewaert@ugent.be (R.A.)
* Correspondence: katja.witschas@ugent.be (K.W.); luc.leybaert@ugent.be (L.L.)
† These authors contributed equally to this work.
‡ These authors share senior authorship.

Abstract: Cx43 hemichannels (HCs) and Panx1 channels are two genetically distant protein families. Despite the lack of sequence homology, Cx43 and Panx1 channels have been the subject of debate due to their overlapping expression and the fact that both channels present similarities in terms of their membrane topology and electrical properties. Using the mimetic peptides Gap19 and ^{10}Panx1, this study aimed to investigate the cross-effects of these peptides on Cx43 HCs and Panx1 channels. The single-channel current activity from stably expressing HeLa-Cx43 and C6-Panx1 cells was recorded using patch-clamp experiments in whole-cell voltage-clamp mode, demonstrating 214 pS and 68 pS average unitary conductances for the respective channels. Gap19 was applied intracellularly while ^{10}Panx1 was applied extracellularly at different concentrations (100, 200 and 500 µM) and the average nominal open probability (NP_o) was determined for each testing condition. A concentration of 100 µM Gap19 more than halved the NP_o of Cx43 HCs, while 200 µM ^{10}Panx1 was necessary to obtain a half-maximal NP_o reduction in the Panx1 channels. Gap19 started to significantly inhibit the Panx1 channels at 500 µM, reducing the NP_o by 26% while reducing the NP_o of the Cx43 HCs by 84%. In contrast ^{10}Panx1 significantly reduced the NP_o of the Cx43 HCs by 37% at 100 µM and by 83% at 200 µM, a concentration that caused the half-maximal inhibition of the Panx1 channels. These results demonstrate that ^{10}Panx1 inhibits Cx43 HCs over the 100–500 µM concentration range while 500 µM intracellular Gap19 is necessary to observe some inhibition of Panx1 channels.

Keywords: Cx43; Panx1; channel gating; single-channel analysis

Citation: Lissoni, A.; Tao, S.; Allewaert, R.; Witschas, K.; Leybaert, L. Cx43 Hemichannel and Panx1 Channel Modulation by Gap19 and ^{10}Panx1 Peptides. *Int. J. Mol. Sci.* **2023**, *24*, 11612. https://doi.org/10.3390/ijms241411612

Academic Editors: Camillo Peracchia and Mario Bortolozzi

Received: 30 June 2023
Revised: 14 July 2023
Accepted: 16 July 2023
Published: 18 July 2023

1. Introduction

Connexins and pannexins are two ubiquitous but distinct protein families forming membrane hemichannels (HCs) and channels in the plasma membrane, respectively. They facilitate the exchange of ions and small molecules (MW $\leq$ 1.5 kDa) between the intracellular and the extracellular compartment upon opening. Among these respective families, connexin-43 (Cx43) and pannexin-1 (Panx1) are the most abundant isotypes in the human body expressed in a wide array of tissues. Panx1 and Cx43 have several common properties, including the following: (i) an analogous tetra-spanning transmembrane topology with cytoplasmic N- and C-termini (NT and CT), two cysteine-containing extracellular loops (ELs) and one cytosolic loop (CL); (ii) a large diameter channel pore in the order of 17–21 Å; (iii) poor ion selectivity; and (iv) channel opening in response to electrical, mechanical and intracellular calcium ($[Ca^{2+}]_i$) elevation. The opening of Panx1 channels and Cx43 HCs is triggered by positive membrane voltages [1,2]. However, Panx1 calcium dependency is currently a matter of debate, since there is also evidence of the channel not being sensitive to moderate $[Ca^{2+}]_i$ elevation in HEK293 cells [3]. Given the structural similarities and overlapping functions of Cx43 and Panx1, the physiological roles of the two proteins are still a subject of debate. Current methods to distinguish between the two channels rely on

electrophysiological approaches (mainly single-channel conductance measurements) and peptide-based inhibitors targeting Cx43 or Panx1. However, single-channel conductance analyses are not without ambiguity, since Cx43 HCs show a fully open conductance in the order of 200–240 pS and a substate of ~80 pS, while Panx1 channel conductance has been reported to be as high as 550 pS in exogenously expressing Xenopus oocytes and between 25 and 100 pS in mammalian cells [4–6]. A second and commonly used strategy is to employ peptides designed to mimic specific regions in the native sequence of connexins and pannexins to interfere with channel function/gating. The mimetic peptides Gap19 and ^{10}Panx1 are widely used inhibitory peptides for Cx43 and Panx1 channels. Gap19 is a nonapeptide mimicking a sequence of nine amino acids on the intracellular loop of Cx43 (KQIEIKKFK), which is crucial for the CT–CL interaction that is a prerequisite for HC gating [7,8]. The ^{10}Panx1 peptide consists of a sequence from the first extracellular loop of Panx1 (WRQAAFVDSY), which is known to affect channel opening [9]. Previous research has shown that the extracellular application of 200 µM Gap19 does not affect ATP release from cells overexpressing Panx1 channels stimulated by high extracellular K^+ depolarizing conditions, while the same concentration of ^{10}Panx1 inhibits ATP release from these cells [10]. In another study, both ^{10}Panx1 and Gap19 were tested in HeLa cells expressing Cx43 or Panx1 channels, providing evidence of good selectivity for both of these peptides at a lower extracellular concentration of 100 µM [11]. However, in these studies, the channel activity was investigated by indirect approaches, such as ATP release and dye uptake experiments, and a direct correlation between mimetic peptide concentrations and single-channel current events is still missing. It is worth noting that ^{10}Panx1 has been reported to partially inhibit Cx46 HC peak currents [12,13], which further emphasizes the need to assess the selectivity of ^{10}Panx1 and Gap19 for Panx1 and Cx43 channels by electrophysiological approaches. Distinguishing between Panx1- and Cx43 HC-related signaling pathways presents a major challenge; therefore, peptide inhibitors of the two channels are often used to determine which channel plays the dominant role. Here, we compared the effects of Gap19 and ^{10}Panx1 on Cx43 and Panx1 channel activities to scrutinize the cross-selectivity of these peptides at concentrations that have been commonly employed. We recorded a large dataset of ~25,000 single-channel opening/closing events from Cx43- and Panx1-expressing mammalian cell lines and analyzed the effects of Gap19 and ^{10}Panx1 on unitary gating transitions from Cx43 HC and Panx1.

2. Results

2.1. Panx1 Channel-Opening Activity Is Concentration-Dependently Inhibited by ^{10}Panx1 Peptide While Gap19 Has No Effect below 500 µM

We used C6 cells stably transfected with Panx1 (C6-Panx1) [14] to determine the single-channel unitary current activity of Panx1 channels upon their exposure to Gap19 and ^{10}Panx1 applied at concentrations of 100, 200 and 500 µM, which have been used in various studies, as summarized in Table 1.

Table 1. Gap19 and ^{10}Panx1 concentrations that have been used to achieve Cx43 and Panx1 channel inhibition, respectively.

Peptide	Concentration (µM)	Application	References
Gap19	100	intracellular	[10,15–17]
	100	extracellular	[11,18–21]
	100	intracellular/extracellular	[22]
	200	intracellular	[23]
	200	extracellular	[10]
	400	intracellular	[10]
	400	extracellular	[24]
	500	extracellular	[10]

Table 1. *Cont.*

Peptide	Concentration (μM)	Application	References
^{10}Panx1	100	extracellular	[9,11,18–20,25–29]
	200	extracellular	[9,10,12,30–37]
	300	extracellular	[38]
	400	extracellular	[39,40]
	500	extracellular	[41]

The representative traces depicted in Figure 1A (enlarged display in Supplementary Figure S1) show unitary Panx1 current activities evoked by repeated (every 40 s) V_m steps from a holding potential of −30 mV to +70 mV (with a duration of 30 s) in voltage-clamp experiments (using whole-cell patch-clamp recording). Under control conditions, a single channel conductance of ~65 pS was observed as determined from the channel transition histograms shown in Figure 1B, i.e., below the 100 pS range, which is typical for voltage-dependent Panx1 channel-opening activity [4–6]. We tested the effect of ^{10}Panx1 and Gap19 on these currents. ^{10}Panx1 was applied extracellularly while Gap19 was applied intracellularly (via a whole-cell recording pipet) as the target interaction sites of these peptides are located outside (^{10}Panx1 is composed of a decapeptide sequence on the first extracellular loop of Panx1 [9], with some evidence pointing to an interaction with the pore of the channel protein [42]) and inside the cell (Gap19 is a mimetic peptide of a sequence on the intracellular loop of Cx43 that interacts with the Cx43 C-terminal tail [7,8,10]), respectively.

Transition histograms report channel transition properties, such as single-channel conductance, but not dwell times in the open or closed states. Figure 1C depicts all-point histograms of the channel activity, showing the event counts in the closed and open states. The largest open-state peak had a ~71 pS single-channel conductance followed by a second smaller peak in the range of the double conductance level, indicating the simultaneous opening of two Panx1 channels. The ~71 pS was not significantly different from the ~65 pS value concluded from the transition analysis. The ^{10}Panx1 peptide clearly decreased the frequency of open-state events, while Gap19 also seemed to have some effect at 200 μM. To better judge the effect of the two peptides, we further quantified the nominal open probability (NP_o) of the Panx1 channels, as shown in Figure 2A. This analysis demonstrated that ^{10}Panx1 significantly reduced the NP_o of the Panx1 channels by 26.0%, 49.5% and 66.0% for the concentrations of 100, 200 and 500 μM, respectively. In contrast, 100 and 200 μM Gap19 did not significantly affect the NP_o of the Panx1 channel; Gap19 did, however, significantly reduce the NP_o at 500 μM (a 26% inhibition; see Figure 2A).

A careful inspection of the experimental traces of the Panx1 channel activity further demonstrated fast-flickering closures in the presence of ^{10}Panx1, which were not observed with Gap19 (Supplementary Figure S2). The flickering frequency increased with the concentration of ^{10}Panx1 (67, 84 and 146 Hz for 100, 200 and 500 μM ^{10}Panx1) and indicated fast ON–OFF gating effects within the channel pore [43].

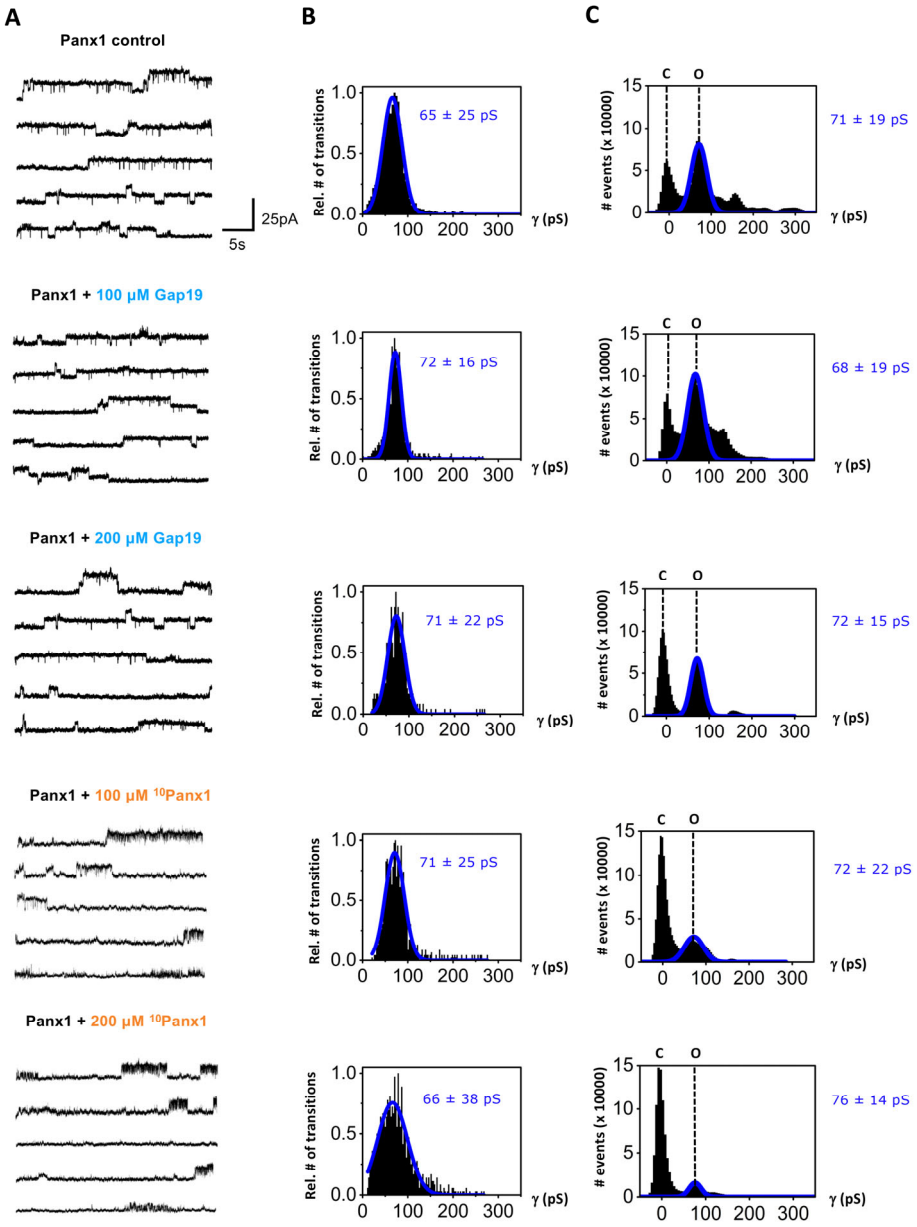

Figure 1. Effect of mimetic peptides Gap19 and ^{10}Panx1 on current activity of Panx1 channels recorded in C6-Panx1 cells. Channel activity was evoked by stepping from a holding potential of −30 mV to +70 mV for 30 s. (**A**) Representative current traces demonstrating channel activity for control conditions and in the presence of Gap19 or ^{10}Panx1. (**B**) Transition histograms demonstrating Gaussian distribution of channel-opening and -closing activity, with indication of the mean ± SD of unitary conductance of the recorded channel transition activity. The conductance values in the presence of the peptides were not significantly different from those under control. The number of transitions is expressed relative to the maximum observed in each of the experimental conditions shown (C6-Panx1 control $\underline{N}$ = 11, N = 30, n = 260; C6-Panx1 + 100 µM Gap19 $\underline{N}$ = 11, N = 12, n = 76; C6-Panx1 + 200 µM Gap19 $\underline{N}$ = 11, N = 9, n = 70; C6-Panx1 + 100 µM ^{10}Panx1 $\underline{N}$ = 11, N = 11, n = 106; C6-Panx1 + 200 µM ^{10}Panx1 $\underline{N}$ = 11, N = 12, n = 116). (**C**) All-point histograms of channel activity showing event counts in the closed (C) and open (O) states expressed as a function of channel conductance. In the presence of the peptide inhibitors, the open-state peaks decreased in height while the closed-state peaks increased, most clearly discernable for ^{10}Panx1 but also to some extent for 200 µM Gap19; significances for these effects at the level of NP_o are given in Figure 2.

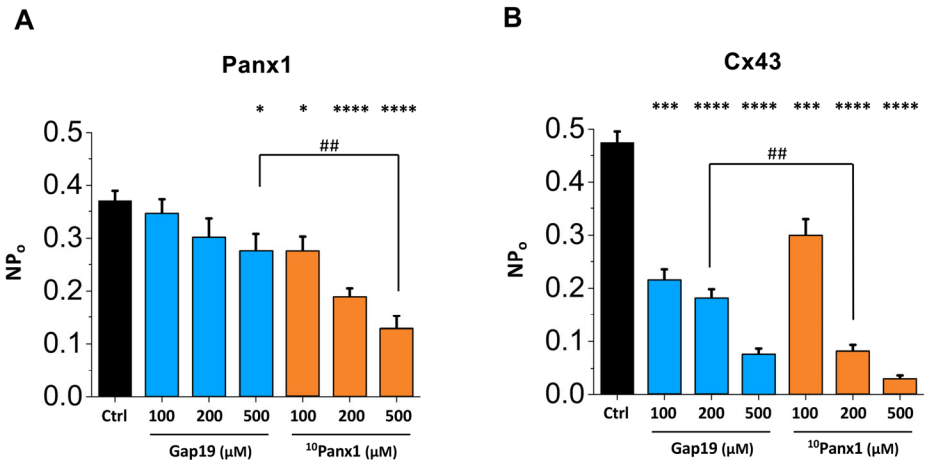

Figure 2. Summary graph of nominal open probability (NP_o) data showing the effect of various Gap19 and ^{10}Panx1 concentrations on Panx1 channels (**A**) and Cx43 HCs (**B**). Statistical analysis by one-way ANOVA with stars (*) indicating comparisons to the control condition (Ctrl) by Dunnett's post-test and number signs (#) indicating significances between Gap19 and ^{10}Panx1 with a Bonferroni post-test (one symbol for $p \leq 0.05$, two symbols for $p \leq 0.01$, three symbols for $p \leq 0.001$ and four symbols for $p \leq 0.0001$). (**A**) C6-Panx1 control = 0.37 ± 0.02 (N = 11, *N* = 30, n = 260); C6-Panx1 + 100 μM Gap19 = 0.34 ± 0.03 (N = 11, *N* = 12, n = 76); C6-Panx1 + 200 μM Gap19 = 0.30 ± 0.03 (N = 11, *N* = 9, n = 70); C6-Panx1 + 500 μM Gap19 = 0.28 ± 0.03 (N = 11, *N* = 10, n = 87); C6-Panx1 + 100 μM ^{10}Panx1 = 0.28 ± 0.03 (N = 11, *N* = 11, n = 106); C6-Panx1 + 200 μM ^{10}Panx1 = 0.19 ± 0.01 (N = 11, *N* = 12, n = 116); C6-Panx1 + 500 μM ^{10}Panx1 = 0.13 ± 0.02 (N = 11, *N* = 11, n = 76). (B) HeLa-Cx43 control = 0.48 ± 0.02 (N = 11, *N* = 23, n = 190); HeLa-Cx43 + 100 μM Gap19 = 0.21 ± 0.02 (N = 11, *N* = 12, n = 98); HeLa-Cx43 + 200 μM Gap19 = 0.18 ± 0.02 (N = 11, *N* = 15, n = 122); HeLa-Cx43 + 500 μM Gap19 = 0.08 ± 0.01 (N = 11, *N* = 12, n = 88); HeLa-Cx43 + 100 μM ^{10}Panx1 = 0.30 ± 0.03 (N = 11, *N* = 12, n = 88); HeLa-Cx43 + 200 μM ^{10}Panx1 = 0.08 ± 0.01 (N = 11, *N* = 11, n = 97); HeLa-Cx43 + 500 μM ^{10}Panx1 = 0.03 ± 0.01 (N = 11, *N* = 8, n = 53).

2.2. Cx43 Hemichannel-Opening Activity Is Inhibited by Gap19 but Also by ^{10}Panx1 at All Concentrations Tested

In the next step, we investigated the effects of the ^{10}Panx1 peptide on Cx43 HC currents. Since the peptide is often used at higher concentrations to inhibit the Panx1 channel (Table 1), we investigated the effect of the ^{10}Panx1 peptide on Cx43 HC currents over a wider concentration range (100, 200 and 500 μM). We used HeLa cells stably expressing Cx43 (HeLa-Cx43), which demonstrated typical Cx43 unitary current activity upon stepping from −30 mV to +70 mV (30 s; Figure 3, enlarged display in Supplementary Figure S3) as previously reported [10]. Cx43 HC gating is characterized by a fully open state in the 200–240 pS range and a subconductance level in the order of 80 pS. In line with previous observations [16], Gap19 reduced the frequency of transitions to the fully open state and increased the propensity of subconductance transitions starting from 100 μM (Figure 3). Interestingly, ^{10}Panx1 exerted a similar effect, increasing the frequency of subconductance transitions while decreasing the frequency of transitions to the fully open state. Note that the subconductance peaks in the transition histograms for the Gap19/^{10}Panx1 peptide conditions look tall (Figure 3B), while the subconductance peaks are hardly visible in the all-point histograms (Figure 3C). This difference is the consequence of the short duration of substate openings (~170 ms on average) while the dwell times for the fully open state are much longer (up to a few seconds) with electrical stimulation as used here. As a result, the impact of increased subconductance gating on the total current flow as well as NP_o is limited. Overall, the NP_o of the Cx43 HC-opening activity clearly demonstrated a concentration-dependent and significant inhibition for Gap19 but also for ^{10}Panx1 (Figure 2B), which reduced the NP_o of the Cx43 HCs by 37% at 100 μM, 83% at 200 μM and 94% at 500 μM (Figure 2B).

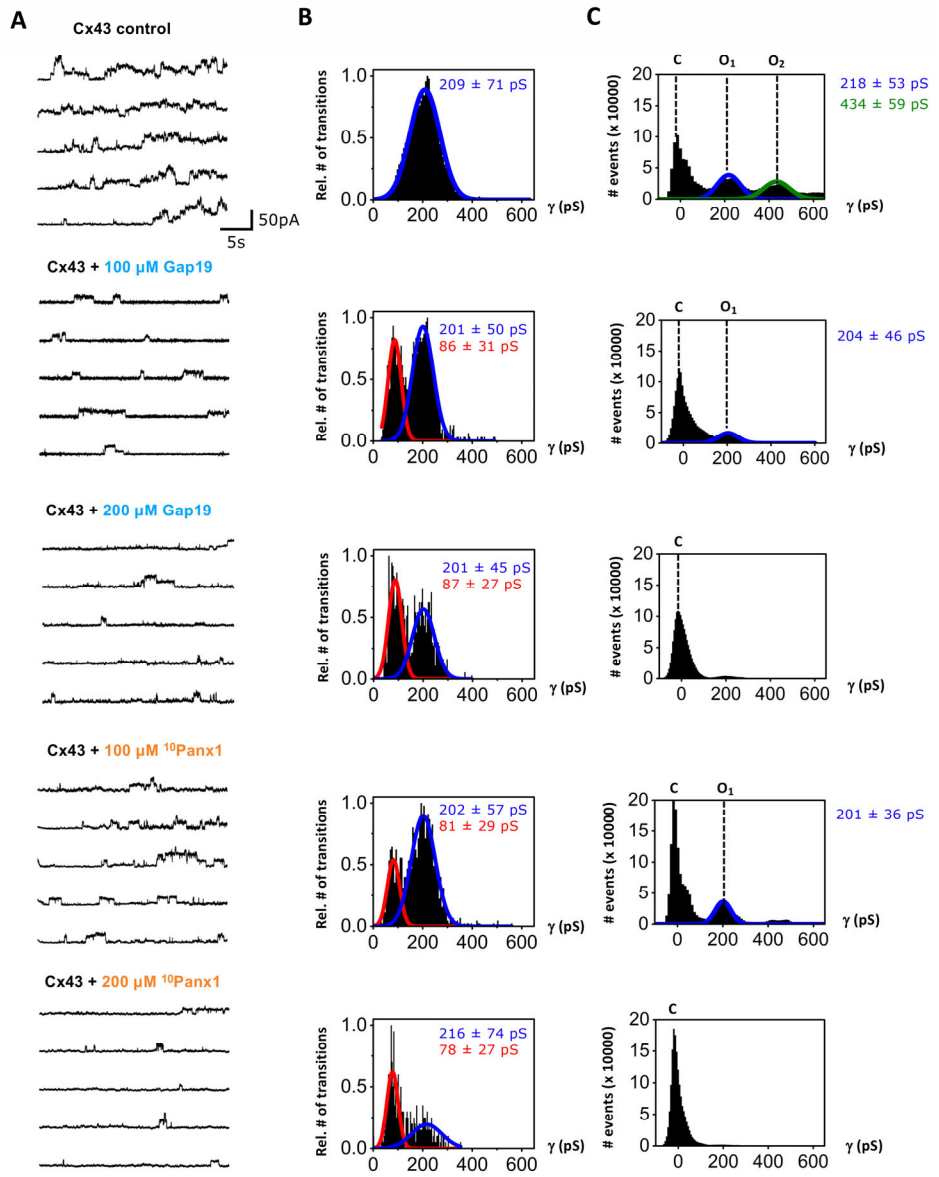

Figure 3. Effect of mimetic peptides Gap19 and ^{10}Panx1 on HC current activity recorded in HeLa-Cx43 cells. Channel activity was evoked by stepping from a holding potential of −30 mV to +70 mV for 30 s. (**A**) Representative current traces demonstrating channel activity for control conditions and in the presence of Gap19 or ^{10}Panx1. (**B**) Transition histograms demonstrating Gaussian distribution of channel opening and closing activity, with indication of the mean ± SD of the recorded channel transition activity. Gap19 as well as ^{10}Panx1 increased gating to the subconductance state as indicated by the red marked peaks. The number of transitions was normalized to the maximum observed in each cluster of the experiment (HeLa-Cx43 control $\underline{N}$ = 11, N = 23, n = 190; HeLa-Cx43 + 100 µM Gap19 $\underline{N}$ = 11, N = 12, n = 98; HeLa-Cx43 + 200 µM Gap19 $\underline{N}$ = 11, N = 15, n = 122; HeLa-Cx43 + 100 µM ^{10}Panx1 $\underline{N}$ = 11, N = 12, n = 88; HeLa-Cx43 + 200 µM ^{10}Panx1 $\underline{N}$ = 11, N = 11, n = 97). (**C**) All-point histograms of channel activity showing event counts in the closed (C) and open states (O_1 and O_2) expressed as a function of channel conductance; O_2 peaked at twice the O_1 conductance, corresponding to stacked (simultaneous) opening of two Cx43 HCs.

3. Discussion

Among the connexin and pannexin families, Cx43 and Panx1 are the most commonly expressed isotypes in the human body. These pore-forming proteins present a strong similarity in terms of their membrane topology, channel gating, permeability profile, modes

of activation and pathophysiological roles (as reviewed in [1,2,44]). As such, conclusions on the contribution of these channels in physiological or pathological responses have been largely based on the effect of peptide inhibitors. This study aimed to investigate the cross-effects of the Gap19 and ^{10}Panx1 peptides on the currents associated with Cx43 HC and Panx1 that are activated by stepping to positive membrane potentials. Our data confirm that Gap19 concentration-dependently inhibits Cx43 HCs (Figure 2B) and acts as a gating modifier, reducing transitions to the fully open state (~210 pS) while increasing the number of transitions to the subconductance state (~80 pS, Figure 3). Gap19 had non-significant effects on Panx1 channel activity at intracellular concentrations up to 200 µM, while at 500 µM, the inhibitory effect on Panx1 was similar to that on 100 µM ^{10}Panx1, causing a ~25% reduction in the NP_o (Figure 2A).

The analysis of Figure 2 indicates that Gap19 applied intracellularly at 100 µM significantly reduces the NP_o of Cx43 HCs without affecting the Panx1 channels. Figure 2A shows that 200 µM extracellular ^{10}Panx1, the concentration most frequently used in published studies (Table 1), brings about the half-maximal inhibition of the Panx1 channel's NP_o. However, this concentration decreases the NP_o of Cx43 HCs by ~83% (Figure 2B; for traces, see Figure 3). Surprisingly, ^{10}Panx1 acted as a gating modifier of the Cx43 HCs at all the concentrations tested, in a similar fashion as previously reported for Gap19 [16], i.e., it reduced the propensity of gating to the main open state but increased the incidence of gating to the HC subconductance state (Figure 3). In contrast, ^{10}Panx1 did not induce the subconductance gating of Panx1 channels (Figure 1). Previous work has suggested that the Gap19 disruption of the interaction between the CT and the CL may be involved in the increased substate gating of Cx43 HCs [16], so it remains to be determined whether ^{10}Panx1 would have any such effects on CT–CL interactions. This brings us to the point of the membrane permeability of the Gap19 and ^{10}Panx1 peptides. Sequence-based estimates of the cell-penetrating potential of candidate peptide sequences using the C2Pred webserver [45] indicated that ^{10}Panx1 has poor membrane permeability. As such, the possibility that the peptide would make its way into the cell and interfere with CT–CL interactions is considered to be low. Possibly, ^{10}Panx1 may indirectly affect CT–CL interactions via peptide interactions with the extracellular loops, thereby impacting the conformational state of the CT and CL structures inside the cell. In fact, such a scenario should also be considered for the Cx43 HC-inhibiting effects of Gap26 and Gap27 which contain amino acid sequences of extracellular loop 1 and 2 from the Cx43 protein.

In the present study, we applied Gap19 to the intracellular compartment via the whole-cell patch-clamp pipette. For comparison, the intracellular Gap19 concentrations approximately corresponded to the extracellular concentrations of membrane-permeable TAT-Gap19, which equilibrates at the two sides of the plasma membrane [10]. Consequently, the Gap19 concentrations used here approximately correspond to comparable concentrations of TAT-Gap19 applied extracellularly. Table 2 demonstrates that TAT-Gap19 concentrations of 100, 200 and 500 µM have been used in published experimental work.

In summary, the present data show that 100–200 µM intracellular Gap19 (equivalent to 100–200 µM TAT-Gap19 applied outside the cell) significantly inhibits Cx43 HCs without affecting Panx1 channel function. Contrastingly, extracellular ^{10}Panx1 more strongly reduces Cx43 HC function than Panx1 channel function at all the concentrations tested, limiting the use of this peptide as a pharmacological tool to identify the involvement of Panx1 channels in cellular function.

To the best of our knowledge, this is the first report on the cross-effects of Gap19 and ^{10}Panx1 based on electrophysiological experiments allowing for a direct readout of Cx43 HC and Panx1 channel function. Our analysis based on a large data set of channel activity provides increased insight into the gating behavior of Cx43 HCs and Panx1 channels. Establishing the gating profiles of these channels is intended to be a starting point for future studies comparing Cx43 HC and Panx1 channel function to identify their respective roles in cell signaling and to drive further experimental research to develop peptides and molecules with optimal target selectivity (as reviewed in [46]). Along this line, novel Panx1 inhibitors

based on a quinoline or indole scaffold have been recently reported to display improved selectivity towards connexins [47,48].

Table 2. Concentrations used for extracellular application of TAT-Gap19.

Peptide	Concentration (μM)	Application	References
TAT-Gap19	100	extracellular	[49–52]
	200	extracellular	[10,24,53–55]
	500	extracellular	[24]

4. Materials and Methods

4.1. Chemicals and Reagents

Ethylene glycol-bis-(β-aminoethyl ether)-N,N,N′,N′-tetraacetic acid (EGTA), 5-tetraethylammonium (TEA)-Cl, pyruvic acid and 4-(2-hydroxyethyl)-1-piperazineethanesulfonic acid (HEPES) were purchased from Sigma-Aldrich (Bornem, Belgium). Gap19 (KQIEIKKFK) and ^{10}Panx1 (WRQAAFVDSY) were synthesized to a purity of >90%.

4.2. Cell Cultures

We used HeLa cells stably transfected with Cx43 (HeLa-Cx43 [56]); endogenous expression of Panx1 is very low [57] or absent [58] in non-transfected HeLa cells. C6 glioma cells stably transfected with Panx1 (C6-Panx1, C-terminally *myc*-tagged; kind gift of Dr Christian C. Naus, University of British Columbia, Canada [14]) were used for the Panx1 channel studies; Cx43 expression is low [59,60] or undetectable [61] in these cells. HeLa cells were maintained in Dulbecco's modified Eagle's medium (DMEM; Invitrogen, Gent, Belgium), and C6 cells were grown in DMEM:Ham's F12 (1:1—Invitrogen, Merelbeke, Belgium), all supplemented with 10% fetal bovine serum (FBS), 2 mM glutamine, 10 U/mL penicillin, 10 μg/mL streptomycin and 0.25 μg/mL fungizone. Stable exogenous expressions were maintained by supplementation of 1 and 3 μg/mL puromycin (Sigma-Aldrich, Bornem, Belgium) for HeLa-Cx43 and C6-Panx1 cells, respectively. Stable transfectants were subcultured into puromycin-free medium 2 days prior to experimentation. Cells were maintained at 37 °C and 10% (HeLa-Cx43) or 5% (C6-Panx1) CO_2.

4.3. Electrophysiological Recordings

All experimental data were obtained with the patch-clamp technique in whole-cell recording mode on HeLa-Cx43 and C6-Panx1 cells. Extracellular solution was composed of the following (in mM): 150 NaCl, 4 CsCl, 2 $CaCl_2$, 2 $MgCl_2$, 2 pyruvic acid, 5 glucose and 5 HEPES at pH of 7.4, while the pipette solution consisted of the following (in mM): 125 CsCl, 10 sodium aspartate (NaAsp), 0.26 $CaCl_2$, 1 $MgCl_2$, 2 EGTA, 10 tetraethylammonium (TEA)-Cl and 5 HEPES at pH 7.2. The free Ca^{2+} concentration of the pipette solution was estimated to be ~50 nM as calculated with WEBMAX (https://somapp.ucdmc.ucdavis.edu/pharmacology/bers/maxchelator/webmaxc/webmaxcS.htm; accessed on 20 September 2020). Whole-cell recording was performed under control conditions and in the presence of Gap19 or ^{10}Panx1. Gap19 was included in the pipette solution, while ^{10}Panx1 was added externally and preincubated for 45 min. Recordings were commenced 2 min after establishment of the whole-cell configuration. Currents were recorded with an EPC 7 PLUS patch-clamp amplifier (HEKA Elektronik, Germany). Unitary current activities were elicited by stepping the cells from a holding potential of −30 mV to a membrane potential (V_m) of +70 mV for 30 s. Data were digitized at 4 KHz using an NI USB-6221 data acquisition device (National Instruments, Austin, TX, USA) and WinWCP acquisition software designed by Dr. J. Dempster (University of Strathclyde, United Kingdom). Measured currents were filtered by a 7-pole Bessel low-pass filter at 1 KHz cut-off frequency. Transition analysis was performed as reported in [16]. Unitary channel conductances were determined from transition histograms as well as from all-point histograms and were obtained by fitting their frequencies to Gaussian distributions. Channel opening activity is

expressed as nominal open probability NP_o, denoting the number of active channels in the patch multiplied by the open probability.

4.4. Statistical Analysis

Data were processed using Clampfit version 11.2 (Molecular Devices, San Jose, USA) and HemiGUI software as previously described [16]. Results are expressed as mean ± SEM (unless otherwise stated), with n giving the number of traces, ***N*** the number of cells, and N the number of experiments on different cell culture dishes. Multiple groups were compared by one-way analysis of variance with post-hoc Dunnett's or Bonferroni multiple comparison tests, making use of GraphPad PRISM 5.0 (GraphPad Software, Inc., La Jolla, CA). Results were considered statistically significant when $p \leq 0.05$ (*; # for $p \leq 0.05$, **; ## for $p \leq 0.01$, ***; ### for $p \leq 0.001$, and ****; #### for $p \leq 0.0001$).

Supplementary Materials: The following supporting information can be downloaded at: https://www.mdpi.com/article/10.3390/ijms241411612/s1.

Author Contributions: Conceptualization, L.L. and A.L.; methodology, A.L., S.T., R.A. and K.W.; software, A.L., S.T. and R.A.; validation, A.L., S.T. and R.A.; formal analysis, A.L., S.T. and R.A.; investigation, A.L., S.T. and R.A.; resources, K.W. and L.L.; data curation, A.L.; writing—original draft preparation, A.L. and K.W.; writing—review and editing, A.L., K.W. and L.L.; visualization, A.L. and S.T.; supervision, K.W. and L.L.; project administration, A.L., K.W. and L.L.; funding acquisition, K.W. and L.L. All authors have read and agreed to the published version of the manuscript.

Funding: Research of the L.L. group is supported by Research Foundation—Flanders (FWO) grants G052718N, G040720N and G063023N. K.W. receives Ghent University funding for her postdoctoral fellowship. K.W. and R.A. are supported by FWO grant G063023N. S.T. acknowledges financial support from the China Scholarship Council (CSC no. 201906170050).

Institutional Review Board Statement: Not applicable.

Informed Consent Statement: Not applicable.

Data Availability Statement: Not applicable.

Acknowledgments: We would like to thank Ellen Cocquyt and Diego De Baere for their superb technical support.

Conflicts of Interest: The authors declare no conflict of interest.

References

1. Giaume, C.; Leybaert, L.; Naus, C.C.; Sáez, J.C. Connexin and Pannexin Hemichannels in Brain Glial Cells: Properties, Pharmacology, and Roles. *Front. Pharmacol.* **2013**, *4*, 88. [CrossRef] [PubMed]
2. D'hondt, C.; Ponsaerts, R.; De Smedt, H.; Bultynck, G.; Himpens, B. Pannexins, Distant Relatives of the Connexin Family with Specific Cellular Functions? *Bioessays* **2009**, *31*, 953–974. [CrossRef]
3. Ma, W.; Hui, H.; Pelegrin, P.; Surprenant, A. Pharmacological Characterization of Pannexin-1 Currents Expressed in Mammalian Cells. *J. Pharmacol. Exp. Ther.* **2009**, *328*, 409–418. [CrossRef]
4. Ma, W.; Compan, V.; Zheng, W.; Martin, E.; North, R.A.; Verkhratsky, A.; Surprenant, A. Pannexin 1 Forms an Anion-Selective Channel. *Pflugers Arch.* **2012**, *463*, 585–592. [CrossRef]
5. Chiu, Y.-H.; Jin, X.; Medina, C.B.; Leonhardt, S.A.; Kiessling, V.; Bennett, B.C.; Shu, S.; Tamm, L.K.; Yeager, M.; Ravichandran, K.S.; et al. A Quantized Mechanism for Activation of Pannexin Channels. *Nat. Commun.* **2017**, *8*, 14324. [CrossRef] [PubMed]
6. Garré, J.M.; Bukauskas, F.F.; Bennett, M.V.L. Single Channel Properties of Pannexin-1 and Connexin-43 Hemichannels and P2X7 Receptors in Astrocytes Cultured from Rodent Spinal Cords. *Glia* **2022**, *70*, 2260–2275. [CrossRef] [PubMed]
7. Leybaert, L.; Lampe, P.D.; Dhein, S.; Kwak, B.R.; Ferdinandy, P.; Beyer, E.C.; Laird, D.W.; Naus, C.C.; Green, C.R.; Schulz, R. Connexins in Cardiovascular and Neurovascular Health and Disease: Pharmacological Implications. *Pharmacol. Rev.* **2017**, *69*, 396–478. [CrossRef] [PubMed]
8. Leybaert, L.; De Smet, M.A.; Lissoni, A.; Allewaert, R.; Roderick, H.L.; Bultynck, G.; Delmar, M.; Sipido, K.R.; Witschas, K. Connexin Hemichannels as Candidate Targets for Cardioprotective and Anti-Arrhythmic Treatments. *J. Clin. Investig.* **2023**, *133*, e168117. [CrossRef]
9. Pelegrin, P.; Surprenant, A. Pannexin-1 Mediates Large Pore Formation and Interleukin-1beta Release by the ATP-Gated P2X7 Receptor. *EMBO J.* **2006**, *25*, 5071–5082. [CrossRef]

10. Wang, N.; De Vuyst, E.; Ponsaerts, R.; Boengler, K.; Palacios-Prado, N.; Wauman, J.; Lai, C.P.; De Bock, M.; Decrock, E.; Bol, M.; et al. Selective Inhibition of Cx43 Hemichannels by Gap19 and Its Impact on Myocardial Ischemia/Reperfusion Injury. *Basic Res. Cardiol.* **2013**, *108*, 309. [CrossRef]
11. Garré, J.M.; Yang, G.; Bukauskas, F.F.; Bennett, M.V.L. FGF-1 Triggers Pannexin-1 Hemichannel Opening in Spinal Astrocytes of Rodents and Promotes Inflammatory Responses in Acute Spinal Cord Slices. *J. Neurosci. Off. J. Soc. Neurosci.* **2016**, *36*, 4785–4801. [CrossRef] [PubMed]
12. Wang, J.; Ma, M.; Locovei, S.; Keane, R.W.; Dahl, G. Modulation of Membrane Channel Currents by Gap Junction Protein Mimetic Peptides: Size Matters. *Am. J. Physiol. Cell Physiol.* **2007**, *293*, C1112-9. [CrossRef] [PubMed]
13. Dahl, G. Gap Junction-Mimetic Peptides Do Work, but in Unexpected Ways. *Cell Commun. Adhes.* **2007**, *14*, 259–264. [CrossRef]
14. Lai, C.P.K.; Bechberger, J.F.; Thompson, R.J.; MacVicar, B.A.; Bruzzone, R.; Naus, C.C. Tumor-Suppressive Effects of Pannexin 1 in C6 Glioma Cells. *Cancer Res.* **2007**, *67*, 1545–1554. [CrossRef] [PubMed]
15. Freitas-Andrade, M.; Wang, N.; Bechberger, J.F.; De Bock, M.; Lampe, P.D.; Leybaert, L.; Naus, C.C. Targeting MAPK Phosphorylation of Connexin43 Provides Neuroprotection in Stroke. *J. Exp. Med.* **2019**, *216*, 916–935. [CrossRef]
16. Lissoni, A.; Wang, N.; Nezlobinskii, T.; De Smet, M.; Panfilov, A.V.; Vandersickel, N.; Leybaert, L.; Witschas, K. Gap19, a Cx43 Hemichannel Inhibitor, Acts as a Gating Modifier That Decreases Main State Opening While Increasing Substate Gating. *Int. J. Mol. Sci.* **2020**, *21*, 7340. [CrossRef]
17. De Smet, M.A.; Lissoni, A.; Nezlobinsky, T.; Wang, N.; Dries, E.; Pérez-Hernández, M.; Lin, X.; Amoni, M.; Vervliet, T.; Witschas, K.; et al. Cx43 Hemichannel Microdomain Signaling at the Intercalated Disc Enhances Cardiac Excitability. *J. Clin. Investig.* **2021**, *131*, e137752. [CrossRef]
18. Sáez, J.C.; Contreras-Duarte, S.; Labra, V.C.; Santibañez, C.A.; Mellado, L.A.; Inostroza, C.A.; Alvear, T.F.; Retamal, M.A.; Velarde, V.; Orellana, J.A. Interferon-γ and High Glucose-Induced Opening of Cx43 Hemichannels Causes Endothelial Cell Dysfunction and Damage. *Biochim. Biophys. Mol. Cell Res.* **2020**, *1867*, 118720. [CrossRef]
19. Orellana, J.A.; Busso, D.; Ramírez, G.; Campos, M.; Rigotti, A.; Eugenín, J.; von Bernhardi, R. Prenatal Nicotine Exposure Enhances Cx43 and Panx1 Unopposed Channel Activity in Brain Cells of Adult Offspring Mice Fed a High-Fat/Cholesterol Diet. *Front. Cell. Neurosci.* **2014**, *8*, 403. [CrossRef]
20. Chávez, C.E.; Oyarzún, J.E.; Avendaño, B.C.; Mellado, L.A.; Inostroza, C.A.; Alvear, T.F.; Orellana, J.A. The Opening of Connexin 43 Hemichannels Alters Hippocampal Astrocyte Function and Neuronal Survival in Prenatally LPS-Exposed Adult Offspring. *Front. Cell. Neurosci.* **2019**, *13*, 460. [CrossRef] [PubMed]
21. Sáez, J.C.; Contreras-Duarte, S.; Gómez, G.I.; Labra, V.C.; Santibañez, C.A.; Gajardo-Gómez, R.; Avendaño, B.C.; Díaz, E.F.; Montero, T.D.; Velarde, V.; et al. Connexin 43 Hemichannel Activity Promoted by Pro-Inflammatory Cytokines and High Glucose Alters Endothelial Cell Function. *Front. Immunol.* **2018**, *9*, 1899. [CrossRef] [PubMed]
22. Gadicherla, A.K.; Wang, N.; Bulic, M.; Agullo-Pascual, E.; Lissoni, A.; De Smet, M.; Delmar, M.; Bultynck, G.; Krysko, D.V.; Camara, A.; et al. Mitochondrial Cx43 Hemichannels Contribute to Mitochondrial Calcium Entry and Cell Death in the Heart. *Basic Res. Cardiol.* **2017**, *112*, 27. [CrossRef] [PubMed]
23. Lillo, M.A.; Himelman, E.; Shirokova, N.; Xie, L.-H.; Fraidenraich, D.; Contreras, J.E. S-Nitrosylation of Connexin43 Hemichannels Elicits Cardiac Stress-Induced Arrhythmias in Duchenne Muscular Dystrophy Mice. *JCI Insight* **2019**, *4*. [CrossRef] [PubMed]
24. Tarzemany, R.; Jiang, G.; Jiang, J.X.; Larjava, H.; Häkkinen, L. Connexin 43 Hemichannels Regulate the Expression of Wound Healing-Associated Genes in Human Gingival Fibroblasts. *Sci. Rep.* **2017**, *7*, 14157. [CrossRef]
25. Diezmos, E.F.; Markus, I.; Perera, D.S.; Gan, S.; Zhang, L.; Sandow, S.L.; Bertrand, P.P.; Liu, L. Blockade of Pannexin-1 Channels and Purinergic P2X7 Receptors Shows Protective Effects Against Cytokines-Induced Colitis of Human Colonic Mucosa. *Front. Pharmacol.* **2018**, *9*, 865. [CrossRef]
26. Weilinger, N.L.; Lohman, A.W.; Rakai, B.D.; Ma, E.M.M.; Bialecki, J.; Maslieieva, V.; Rilea, T.; Bandet, M.V.; Ikuta, N.T.; Scott, L.; et al. Metabotropic NMDA Receptor Signaling Couples Src Family Kinases to Pannexin-1 during Excitotoxicity. *Nat. Neurosci.* **2016**, *19*, 432–442. [CrossRef]
27. Karpuk, N.; Burkovetskaya, M.; Fritz, T.; Angle, A.; Kielian, T. Neuroinflammation Leads to Region-Dependent Alterations in Astrocyte Gap Junction Communication and Hemichannel Activity. *J. Neurosci. Off. J. Soc. Neurosci.* **2011**, *31*, 414–425. [CrossRef]
28. Basu, M.; Gupta, P.; Dutta, A.; Jana, K.; Ukil, A. Increased Host ATP Efflux and Its Conversion to Extracellular Adenosine Is Crucial for Establishing Leishmania Infection. *J. Cell Sci.* **2020**, *133*. [CrossRef]
29. Thompson, R.J.; Jackson, M.F.; Olah, M.E.; Rungta, R.L.; Hines, D.J.; Beazely, M.A.; MacDonald, J.F.; MacVicar, B.A. Activation of Pannexin-1 Hemichannels Augments Aberrant Bursting in the Hippocampus. *Science* **2008**, *322*, 1555–1559. [CrossRef]
30. Orellana, J.A.; Moraga-Amaro, R.; Díaz-Galarce, R.; Rojas, S.; Maturana, C.J.; Stehberg, J.; Sáez, J.C. Restraint Stress Increases Hemichannel Activity in Hippocampal Glial Cells and Neurons. *Front. Cell. Neurosci.* **2015**, *9*, 102. [CrossRef]
31. Luu, R.; Valdebenito, S.; Scemes, E.; Cibelli, A.; Spray, D.C.; Rovegno, M.; Tichauer, J.; Cottignies-Calamarte, A.; Rosenberg, A.; Capron, C.; et al. Pannexin-1 Channel Opening Is Critical for COVID-19 Pathogenesis. *iScience* **2021**, *24*, 103478. [CrossRef] [PubMed]
32. Orellana, J.A.; Froger, N.; Ezan, P.; Jiang, J.X.; Bennett, M.V.L.; Naus, C.C.; Giaume, C.; Sáez, J.C. ATP and Glutamate Released via Astroglial Connexin 43 Hemichannels Mediate Neuronal Death through Activation of Pannexin 1 Hemichannels. *J. Neurochem.* **2011**, *118*, 826–840. [CrossRef] [PubMed]

33. Momboisse, F.; Olivares, M.J.; Báez-Matus, X.; Guerra, M.J.; Flores-Muñoz, C.; Sáez, J.C.; Martínez, A.D.; Cárdenas, A.M. Pannexin 1 Channels: New Actors in the Regulation of Catecholamine Release from Adrenal Chromaffin Cells. *Front. Cell. Neurosci.* **2014**, *8*, 270. [CrossRef]
34. Lohman, A.W.; Leskov, I.L.; Butcher, J.T.; Johnstone, S.R.; Stokes, T.A.; Begandt, D.; DeLalio, L.J.; Best, A.K.; Penuela, S.; Leitinger, N.; et al. Pannexin 1 Channels Regulate Leukocyte Emigration through the Venous Endothelium during Acute Inflammation. *Nat. Commun.* **2015**, *6*, 7965. [CrossRef]
35. Shoji, K.F.; Sáez, P.J.; Harcha, P.A.; Aguila, H.L.; Sáez, J.C. Pannexin1 Channels Act Downstream of P2X 7 Receptors in ATP-Induced Murine T-Cell Death. *Channels* **2014**, *8*, 142–156. [CrossRef]
36. Xiang, X.; Langlois, S.; St-Pierre, M.-E.; Barré, J.F.; Grynspan, D.; Purgina, B.; Cowan, K.N. Pannexin 1 Inhibits Rhabdomyosarcoma Progression through a Mechanism Independent of Its Canonical Channel Function. *Oncogenesis* **2018**, *7*, 89. [CrossRef] [PubMed]
37. Adamiak, M.; Abdel-Latif, A.; Bujko, K.; Thapa, A.; Anusz, K.; Tracz, M.; Brzezniakiewicz-Janus, K.; Ratajczak, J.; Kucia, M.; Ratajczak, M.Z. Nlrp3 Inflammasome Signaling Regulates the Homing and Engraftment of Hematopoietic Stem Cells (HSPCs) by Enhancing Incorporation of CXCR4 Receptor into Membrane Lipid Rafts. *Stem Cell Rev. Rep.* **2020**, *16*, 954–967. [CrossRef]
38. Sorge, R.E.; Trang, T.; Dorfman, R.; Smith, S.B.; Beggs, S.; Ritchie, J.; Austin, J.-S.; Zaykin, D.V.; Vander Meulen, H.; Costigan, M.; et al. Genetically Determined P2X7 Receptor Pore Formation Regulates Variability in Chronic Pain Sensitivity. *Nat. Med.* **2012**, *18*, 595–599. [CrossRef]
39. Dossi, E.; Blauwblomme, T.; Moulard, J.; Chever, O.; Vasile, F.; Guinard, E.; Le Bert, M.; Couillin, I.; Pallud, J.; Capelle, L.; et al. Pannexin-1 Channels Contribute to Seizure Generation in Human Epileptic Brain Tissue and in a Mouse Model of Epilepsy. *Sci. Transl. Med.* **2018**, *10*. [CrossRef]
40. Brough, D.; Pelegrin, P.; Rothwell, N.J. Pannexin-1-Dependent Caspase-1 Activation and Secretion of IL-1beta Is Regulated by Zinc. *Eur. J. Immunol.* **2009**, *39*, 352–358. [CrossRef]
41. Pelegrin, P.; Surprenant, A. Pannexin-1 Couples to Maitotoxin- and Nigericin-Induced Interleukin-1beta Release through a Dye Uptake-Independent Pathway. *J. Biol. Chem.* **2007**, *282*, 2386–2394. [CrossRef] [PubMed]
42. Caufriez, A.; Lamouroux, A.; Martin, C.; Iaculli, D.; Ince Ergüç, E.; Gozalbes, R.; Mayan, M.D.; Kwak, B.R.; Tabernilla, A.; Vinken, M.; et al. Determination of Structural Features That Underpin the Pannexin1 Channel Inhibitory Activity of the Peptide (10)Panx1. *Bioorg. Chem.* **2023**, *138*, 106612. [CrossRef] [PubMed]
43. Wonderlin, W.F.; French, R.J.; Arispe, N.J. Recording and Analysis of Currents from Single Ion Channels. In *Neurophysiological Techniques: Basic Methods and Concepts*; Boulton, A.A., Baker, G.B., Vanderwolf, C.H., Eds.; Humana Press: Totowa, NJ, USA, 1990; pp. 35–142. ISBN 978-1-59259-619-5.
44. Scemes, E.; Suadicani, S.O.; Dahl, G.; Spray, D.C. Connexin and Pannexin Mediated Cell-Cell Communication. *Neuron Glia Biol.* **2007**, *3*, 199–208. [CrossRef] [PubMed]
45. Tang, H.; Su, Z.-D.; Wei, H.-H.; Chen, W.; Lin, H. Prediction of Cell-Penetrating Peptides with Feature Selection Techniques. *Biochem. Biophys. Res. Commun.* **2016**, *477*, 150–154. [CrossRef] [PubMed]
46. Koval, M.; Schug, W.J.; Isakson, B.E. Pharmacology of Pannexin Channels. *Curr. Opin. Pharmacol.* **2023**, *69*, 102359. [CrossRef]
47. Crocetti, L.; Giovannoni, M.P.; Guerrini, G.; Lamanna, S.; Melani, F.; Bartolucci, G.; Pallecchi, M.; Paoli, P.; Lippi, M.; Wang, J.; et al. Design, Synthesis and Pharmacological Evaluation of New Quinoline-Based Panx-1 Channel Blockers. *Int. J. Mol. Sci.* **2023**, *24*, 2022. [CrossRef]
48. Crocetti, L.; Guerrini, G.; Puglioli, S.; Giovannoni, M.P.; Di Cesare Mannelli, L.; Lucarini, E.; Ghelardini, C.; Wang, J.; Dahl, G. Design and Synthesis of the First Indole-Based Blockers of Panx-1 Channel. *Eur. J. Med. Chem.* **2021**, *223*, 113650. [CrossRef]
49. Ramadan, R.; Vromans, E.; Anang, D.C.; Goetschalckx, I.; Hoorelbeke, D.; Decrock, E.; Baatout, S.; Leybaert, L.; Aerts, A. Connexin43 Hemichannel Targeting With TAT-Gap19 Alleviates Radiation-Induced Endothelial Cell Damage. *Front. Pharmacol.* **2020**, *11*, 212. [CrossRef]
50. Barnett, S.D.; Asif, H.; Anderson, M.; Buxton, I.L.O. Novel Tocolytic Strategy: Modulating Cx43 Activity by S-Nitrosation. *J. Pharmacol. Exp. Ther.* **2021**, *376*, 444–453. [CrossRef]
51. Figueroa, V.A.; Jara, O.; Oliva, C.A.; Ezquer, M.; Ezquer, F.; Retamal, M.A.; Martínez, A.D.; Altenberg, G.A.; Vargas, A.A. Contribution of Connexin Hemichannels to the Decreases in Cell Viability Induced by Linoleic Acid in the Human Lens Epithelial Cells (HLE-B3). *Front. Physiol.* **2019**, *10*, 1574. [CrossRef]
52. Chen, Y.; Wang, L.; Zhang, L.; Chen, B.; Yang, L.; Li, X.; Li, Y.; Yu, H. Inhibition of Connexin 43 Hemichannels Alleviates Cerebral Ischemia/Reperfusion Injury via the TLR4 Signaling Pathway. *Front. Cell. Neurosci.* **2018**, *12*, 372. [CrossRef]
53. Abudara, V.; Bechberger, J.; Freitas-Andrade, M.; De Bock, M.; Wang, N.; Bultynck, G.; Naus, C.C.; Leybaert, L.; Giaume, C. The Connexin43 Mimetic Peptide Gap19 Inhibits Hemichannels without Altering Gap Junctional Communication in Astrocytes. *Front. Cell. Neurosci.* **2014**, *8*, 306. [CrossRef] [PubMed]
54. Li, W.; Bao, G.; Chen, W.; Qiang, X.; Zhu, S.; Wang, S.; He, M.; Ma, G.; Ochani, M.; Al-Abed, Y.; et al. Connexin 43 Hemichannel as a Novel Mediator of Sterile and Infectious Inflammatory Diseases. *Sci. Rep.* **2018**, *8*, 166. [CrossRef] [PubMed]
55. Walrave, L.; Pierre, A.; Albertini, G.; Aourz, N.; De Bundel, D.; Van Eeckhaut, A.; Vinken, M.; Giaume, C.; Leybaert, L.; Smolders, I. Inhibition of Astroglial Connexin43 Hemichannels with TAT-Gap19 Exerts Anticonvulsant Effects in Rodents. *Glia* **2018**, *66*, 1788–1804. [CrossRef]
56. Elfgang, C.; Eckert, R.; Lichtenberg-Fraté, H.; Butterweck, A.; Traub, O.; Klein, R.A.; Hülser, D.F.; Willecke, K. Specific Permeability and Selective Formation of Gap Junction Channels in Connexin-Transfected HeLa Cells. *J. Cell Biol.* **1995**, *129*, 805–817. [CrossRef]

57. Huang, Y.; Grinspan, J.B.; Abrams, C.K.; Scherer, S.S. Pannexin1 Is Expressed by Neurons and Glia but Does Not Form Functional Gap Junctions. *Glia* **2007**, *55*, 46–56. [CrossRef] [PubMed]
58. Zappalà, A.; Cicero, D.; Serapide, M.F.; Paz, C.; Catania, M.V.; Falchi, M.; Parenti, R.; Pantò, M.R.; La Delia, F.; Cicirata, F. Expression of Pannexin1 in the CNS of Adult Mouse: Cellular Localization and Effect of 4-Aminopyridine-Induced Seizures. *Neuroscience* **2006**, *141*, 167–178. [CrossRef]
59. Naus, C.C.; Bechberger, J.F.; Caveney, S.; Wilson, J.X. Expression of Gap Junction Genes in Astrocytes and C6 Glioma Cells. *Neurosci. Lett.* **1991**, *126*, 33–36. [CrossRef]
60. Zhu, D.; Caveney, S.; Kidder, G.M.; Naus, C.C. Transfection of C6 Glioma Cells with Connexin 43 CDNA: Analysis of Expression, Intercellular Coupling, and Cell Proliferation. *Proc. Natl. Acad. Sci. USA* **1991**, *88*, 1883–1887. [CrossRef]
61. Wang, N.; De Bock, M.; Antoons, G.; Gadicherla, A.K.; Bol, M.; Decrock, E.; Evans, W.H.; Sipido, K.R.; Bukauskas, F.F.; Leybaert, L. Connexin Mimetic Peptides Inhibit Cx43 Hemichannel Opening Triggered by Voltage and Intracellular Ca^{2+} Elevation. *Basic Res. Cardiol.* **2012**, *107*, 304. [CrossRef]